Pergamon

SCIENCE DIRECT

Bioorganic & Medicinal Chemistry Letters 13 (2003) 4355–4359

BIOORGANIC & MEDICINAL CHEMISTRY LETTERS

Successful Shape-Based Virtual Screening: The Discovery of a Potent Inhibitor of the Type I TGFβ Receptor Kinase (TβRI)

Juswinder Singh,* Claudio E. Chuaqui, P. Ann Boriack-Sjodin, Wen-Cherng Lee, Timothy Pontz, Michael J. Corbley, H.-Kam Cheung, Robert M. Arduini, Jonathan N. Mead, Miki N. Newman, James L. Papadatos, Scott Bowes, Serene Josiah and Leona E. Ling

Biogen Inc., 12 Cambridge Center, Cambridge, MA 02142, USA

Accepted 16 September 2003

Abstract—We describe the discovery, using shape-based virtual screening, of a potent, ATP site-directed inhibitor of the TβRI kinase, an important and novel drug target for fibrosis and cancer. The first detailed report of a TβRI kinase small molecule co-complex confirms the predicted binding interactions of our small molecule inhibitor, which stabilizes the inactive kinase conformation. Our results validate shape-based screening as a powerful tool to discover useful leads against a new drug target.

TGFβ1, TGFβ2 and TGFβ3 are multifunctional cytokines that play a critical role in the regulation of production, degradation and accumulation of extracellular matrix proteins.[1,2] The TGFβ pathway plays a pivotal role in progressive fibrotic diseases of the lung, liver and kidney that are major causes of morbidity and mortality, and represents an exciting target for the development of novel anti-fibrotic agents.[3–5]

The complex of TGFβ with the TGFβ Type II receptor (TβRII) binds and activates TβRI by phosphorylating the GS region. This activated complex is able to bind and phosphorylate Smad substrates which are then able to translocate to the nucleus and induce TGFβ dependent gene expression.[6] The X-ray crystal structure of the unphosphorylated cytoplasmic region of TβRI has been determined in complex with FKBP12, a protein inhibitor of the TGFβ pathway.[7] The crystal structure revealed FKBP12 bound to the regulatory GS region of the receptor, which would prevent phosphorylation by the TβRII. This structure forms the basis for a virtual screening strategy to discover novel inhibitors.

Virtual screening holds great promise as an inexpensive and fast alternative to high-throughput screening (HTS) to discover useful starting points for drug discovery projects.[8] The binding of a ligand to a receptor is driven in part by complementarities in shape and physicochemical interactions. Structure-based virtual screening focuses on using the target structure and is exemplified by receptor-based docking methods such as DOCK, FlexX, ICM, and GOLD.[9] An alternative virtual screening approach is to develop a pharmacophore query which represents the 3-D arrangement of a set of chemical features/functional groups from an inhibitor that are critical to interacting with the receptor.[10] Pharmacophore approaches usually describe pharmacophore triangles and ignore the shape of the molecule. More recently, several new approaches have been described for pharmacophore screening that enable both shape and pharmacophoric information to be included in the search query.[11,12]

The starting point for this virtual screen was SB203580, which has a reported IC_{50} of 30 μM against TβRI.[13] This 2,4,5-triarylimidazole was used to construct a 3-D query. Our objective was to search for molecules with alternative chemistries to the triarylimidazole in a commercially available database that satisfied five pharmacophore features and also had a similar shape (Fig. 1). The pharmacophoric query was built using the HypoHypothesis workbench within Catalyst[14] using the conformation of SB203580 reported in the X-ray complex with p38 (pdbcode 1a9u). The shape component of the query was built using the CatShape module within Catalyst. This query was used to search a multi-conformational Catalyst database, which was built using the

*Corresponding author. Fax: +1-617-679-2616; e-mail: juswinder_singh@biogen.com

0960-894X/$ - see front matter © 2003 Elsevier Ltd. All rights reserved.
doi:10.1016/j.bmcl.2003.09.028

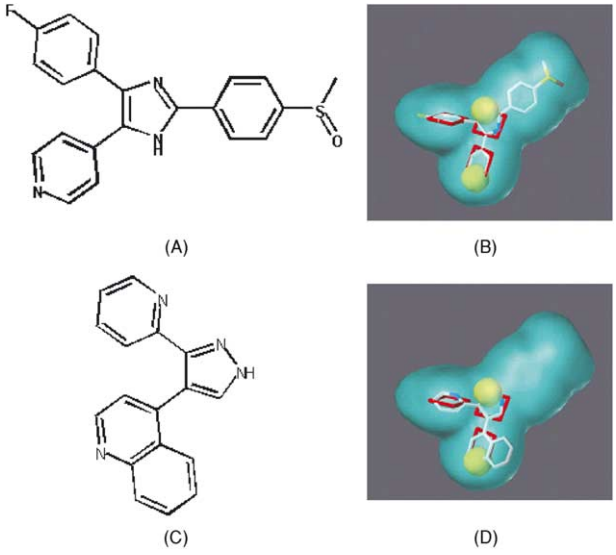

Figure 1. Lead discovery by virtual screening: (A) 2-D chemical structure of SB203580; (B) Representation of shape-based query based upon X-ray bound conformation of SB203580. The shape component of the query is shown in blue, while the aromatic features are shown as red planes, and the hydrogen-bond acceptors as green spheres. The molecule is shown as a stick representation and is colored by atom type; (C) 2-D chemical structure of HTS466284; (D) Virtual screening hit HTS466284 fitted to the shape-based query. The hit satisfies the shape component of the query and all the aromatic and hydrogen-bond acceptor features.

Fast option with the MAXCONFS option set to 250 and the energy threshold set to 15 kcal/mol.

Our choice of pharmacophore features was based upon a derived alignment of p38-SB203580 into the ATP site of TβRI using Combinatorial Extension ((http://cl.sdsc.edu/ce.html). Two hydrogen-bond acceptor features were predicted to interact with the side chain amino group of Lys232 and the backbone NH of His283. This lysine position is strictly conserved across the kinase family and is involved in coordination of the triphosphate moiety of ATP, while the backbone NH is involved in binding of the adenine moiety of ATP. The majority of kinase inhibitors that have been deposited in the protein databank form interactions with these positions (Singh, data not shown). Three of the four aromatic centers in SB203580 were selected as being required. The fourth aromatic ring center was not explicitly selected in the query since our model suggested this could be substituted by a non-aromatic ring system. These query pharmacophoric features were assigned a tolerance of 2 Å. Molecules in the multi-conformational Catalyst database were checked to see if they matched pharmacophore features and also the shape component of the query using a similarity in their shape volumes, as defined by a similarity tolerance value. By setting this value to 0.5 we indicated that half of the volume grid points must match between the target and query for a hit to be returned from the database. The grid resolution for the screen was set to the default value of 1 Å.

The query identified 87 compounds from a commercially available database of 200,000 compounds as satisfying both the shape constraint and pharmacophore features. The molecules identified included triarylimidazoles similar to SB203580 upon which the query was based, in addition to a broad range of templates that were structurally diverse from the starting molecule. A potent inhibitor, designated HTS466284, was identified which inhibited autophosphorylation with an IC_{50} of 27 nM (Fig. 2a). To determine whether HTS466284 was a competitor of ATP, autophosphorylation activity was measured as a function of ATP concentration for several concentrations of the inhibitor. A Lineweaver–Burk plot of the data yielded a family of lines which converged on the Y-axis, which is diagnostic of substrate (ATP) competitive inhibition. To determine the dissociation constant K_d of the inhibitor for the kinase, a saturation binding experiment was performed. Increasing concentrations of a tritiated version of HTS466284 were added to immobilized TβR1 kinase as shown in Fig. 2b. The resulting points were fit to a quadratic curve by non-linear regression, yielding a K_d of 5 nM (range = 4–6 nM, $n = 3$).

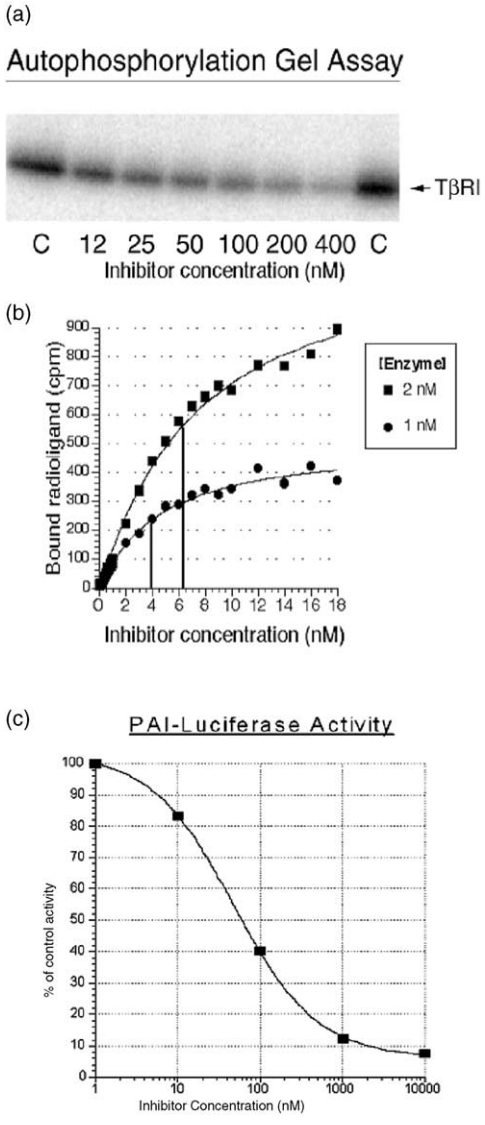

Figure 2. (a) HTS466284 inhibits TβRI autophosphorylation; (b) Determination of dissociation constant K_d by saturation radioligand binding; (c) HTS466284 blocks induction of TGFβ-inducible gene reporter PAI-luciferase in HepG2 cells.

HTS466284 was then tested for activity in cells grown in culture. HTS466284 inhibited TGFβ-induced expression of a transfected PAI-luciferase reporter in a dose-dependent manner (Fig. 2c) with an IC_{50} of 60 nM (range = 50–76 nM, $n = 3$). HTS466284 had no effect on cell viability up to 10 μM, the highest concentration tested. Together the results indicate that HTS466284 is a potent, non-toxic inhibitor of TßRI both in vitro and in cell culture.

In order to validate our virtual screening hypothesis we determined the structure of the complex of TβRI with HTS466284 by X-ray crystallography. The structure of TβRI has the canonical kinase fold consisting of a predominantly β-sheet N-terminal domain and a helical C-terminal domain. This crystal structure contains five monomers arranged in a ring with 5-fold non-crystallographic symmetry. The monomers are extremely similar to each other with an average RMS deviation between Cα positions of 0.57 Å. Variation is seen in the structures at αGS1, αF-αG and αG-αH loop regions of the C-terminal domain, all of which are regions that are involved in crystal contacts. In addition, variation is seen between the monomers at the loop region between αGS1 and αGS2, the activation segment and in the E6 loop which are all solvent exposed and not involved in crystal contacts. Electron density for the activation segment of each monomer is extremely weak and residues have been removed from the model in 3 of 5 monomers. The differences between the monomers are not in regions in contact with the inhibitor.

The binding site for ATP is located in the cleft between the two domains and the inhibitor occupies this site as expected (Fig. 3). HTS466284 binds in the predicted orientation and satisfies the expected aromatic and hydrogen-bond acceptor features as defined by our shape query. The high potency can be rationalized in terms of distinct hydrogen bonding and van der Waals interactions between the inhibitor and TβRI identified in the X-ray structure. The pyrazole N2 and quinoline nitrogen form hydrogen bonds with Lys232 side chain nitrogen and His283 backbone amide NH, respectively, as expected since these two protein hydrogen-bond interactions are common in known kinase inhibitor complexes (Singh, data not shown). There are two additional hydrogen-bonds seen in the complex that were not part of the query. The first involves the N1 of the pyrazole ring, which acts as a hydrogen bond donor with one of the carboxylate oxygens from Asp351. The second additional interaction involves the 2-pyridyl nitrogen that forms a water-mediated network of hydrogen bonds with the enzyme. The inhibitor and receptor form a tetrahedral complex with the water molecule. The water molecule donates hydrogen bonds to the pyridyl nitrogen of HTS466284 and the carboxyl oxygen of Glu245 and accepts hydrogen bonds from the phenol of Tyr249 and the backbone NH of Asp351 (Fig. 4).

The quinoline, pyrazole and pyridyl rings satisfy the expected aromatic interactions as defined by the shape query. The quinoline moiety of HTS466284 binds in an analogous position to that occupied by the adenine group of ATP in known ATP-kinase complexes. In addition, residues Ile211, Ala230, and Leu340, on either side of the plane of the quinoline ring make van der Waals contacts with the inhibitor. The pyridine ring of HTS466284 is inserted into a hydrophobic pocket formed between αC and β1-β4 of the ATP binding site making contacts with the following cluster of residues: Ala230, Lys232, Leu260, Leu278, Val279 and Ser280.

TβRI has been previously crystallized in complex with a small molecule inhibitor, NPC-30345. Although no detailed small molecule binding information was reported for this complex, we can use the structure to compare the effects of the inhibitors on the protein structure. Our crystal structure closely resembles the FKBP12-TβRI and NPC-30345-TβRI crystal structures, which have

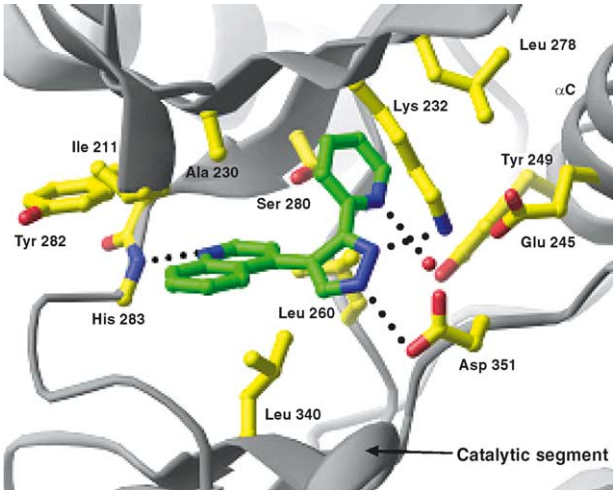

Figure 3. Inhibitor interactions in the TβRI active site. HTS466284 (green) is shown with contacting residues in the active site (yellow) using the program RIBBONS.[15] Hydrogen bond interactions made by the inhibitor are shown as dashed lines. The water molecule is indicated as a red sphere.

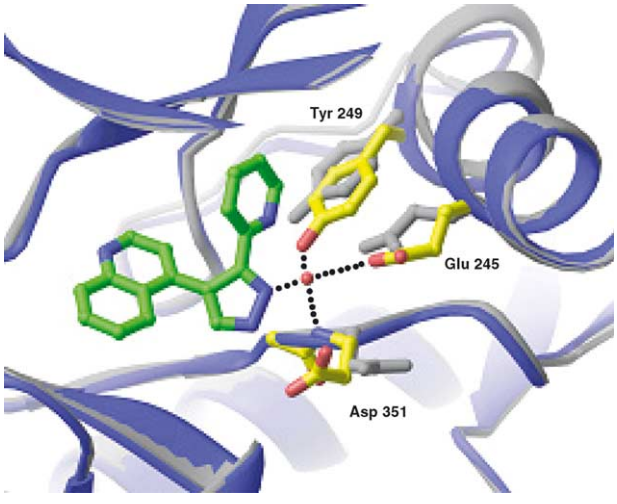

Figure 4. Water molecule in the active site. The water molecule (red sphere) hydrogen bonds to the inhibitor (green) and 3 residues of the protein (yellow): Tyr249, Glu245, and Asp351. The corresponding residues in the NPC-30345-TβRI are also shown (grey; pdbcode 1IAS). The movement of Glu245 and Tyr249 causes a change in the helical structure at the end of helix αC of the HTS466284 complex.

Table 1. Summary of crystallographic data

Data Collection		Refinement	
Resolution (Å)	50–2.9 (3.0–2.9)[a]	Total number of atoms	13274
No. of Reflections (total/unique)	488001/65569	R_{factor}/R_{free} [c]	0.233/0.285
Completeness (%)	97.5 (97.1)	Rmsd for bonds (Å)	0.008
I/σ	16.9 (3.2)	Rmsd for angles (deg)	1.50
R_{sym} [b]	0.070 (0.370)		

[a]Numbers in parentheses refer to outer resolution shell.
[b]$R_{sym} = \Sigma\ |I - <I>| / \Sigma\ I$, where I is the integrated intensity of a given reflection.
[c]R value = $\Sigma\ |F(obs) - F(calc)| / \Sigma\ F(obs)$, where F(calc) represents the structure factor amplitudes obtained from back transformation of the model. 10% of the data was used in calculating R_{free}.

been classed by Huse et al. as inactive conformations of the kinase through comparisons to the crystal structure of an active kinase structure, PKA. In the FKBP12 complex with TβRI, the αC helix is caged between the activation segment and GS regulatory region, which prevents the kinase from adopting the active conformation. The activation segment of the FKBP12 complex is pinned to αC Ser241 via hydrogen bonds from Arg372 and Asn370. Arg372 from the activation segment is locked onto the catalytic segment via a hydrogen bond with Asp351. In contrast, for both small molecule complexes, the activation segment is no longer coupled to αC helix and is directed away from the catalytic center. The structural variation seen between the monomers suggests that the region is flexible. The GS loop adopts a non-inhibitory conformation, which is no longer inserted between β4 and αC helix, therefore not restricting the rotation of αC. However, for both small molecule complexes, the inactive conformation of the kinase remains, which is probably a consequence of the stabilization of this form by the interactions with the small molecule.

Comparisons of the structures of TβRI-NPC30345 and TβRI-HTS466284 show that they are very similar, with an RMS deviation of 1.04 Å over the Cα positions across the entire pentamer, and many of the differences seen are similar to those within the monomers for each of the complexes. There are several notable changes that are attributable to small molecule binding. The C-terminal end of αC helix is directed inwards, towards the catalytic center, where Tyr249 and Glu245 are coordinated to our inhibitor via a water molecule (Fig 4). Interestingly, the final turn of αC is missing in our structure relative to both the FKBP12 and NPC-30345 complexes, which suggests that this water-mediated interaction is formed at the expense of the helical structure of this region of αC. Another key difference is that Asp351 is directed inwards towards the small molecule, forming a hydrogen-bonding interaction, in contrast to the NPC-30345 complex, which is directed away from the catalytic center in a similar conformation to the FKBP12 complex. Finally, Phe216, which is packed down towards the small molecule in the NPC-30345 complex, is directed away from the inhibitor in the HTS466284 complex (Table 1).

The crystal structures of the three known TβRI kinase inhibitor complexes adopt very similar folds and all exist in an inactive conformation and would be unable to accommodate ATP binding and substrate phosphorylation. The two small molecule inhibitor complexes are more similar to each other than to the FKBP12 bound form of TβRI. Significant differences exist in the GS region and activation segment between the FKBP12 and small molecule complexes, which in part reflect the ability of FKBP12 to stabilize the inhibitory conformation of the regulatory GS region of the kinase. Our results suggest that both small molecules are able to stabilize the inactive conformation of TβR1 in similar ways; however, differences do exist at the level of side chain and backbone interactions.

Using virtual screening, we have successfully identified a novel and potent inhibitor of the TβRI pathway. Our results confirm shape-based virtual screening as a powerful tool to discover novel inhibitors of the protein kinase family, and further validate virtual screening as an inexpensive and efficient means for lead discovery. HTS466284 will be a useful tool to study TGFβ signaling in vitro and in vivo.

Acknowledgements

We thank Adrian Whitty, Dongyu Sun, Konrad Miatkowski, Kristy Favell, Darren Baker, Sayre Neufeld, Craig Ogata and the X4A staff at Brookhaven National Laboratories. We also thank Herman van Vlijmen, Abhas Gupta, Donovan Chin, Rainer Fuchs, Kumud Singh and Russell Petter for critical review of the manuscript.

Supporting Information Available: Experimental details including expression and purification of enzyme, kinase assays, ATP competition, cellular assays, X-ray data collection and model building and refinement

References and Notes

1. Massague, J. *Annu. Rev. Biochem.* **1998**, *67*, 753.
2. Massague, J. B.; Blain, S. W.; Lo, R. S. *Cell* **2000**, *103*, 295.

3. Franklin, T. J. *Int. J. Biochem. Cell Biol.* **1997**, *29*, 78.
4. Border, W. A.; Roslahti, E. *J. Clin. Invest.* **1992**, *90*, 1.
5. Laping, N. J. *IDRUGS* **1999**, *2*, 907.
6. Heldin, C. H.; Miyazono, K.; ten Dijke, P. *Nature* **1997**, *390*, 465.
7. Huse, M.; Chen, Y. G.; Massague, J.; Kuriyan, J. *Cell* **1999**, *96*, 425.
8. Bajorath, J. *Nature Rev. Drug Discov.* **2002**, *1*, 882.
9. Joseph-McCarthy, D. *Pharmacol. Therap.* **1999**, *84*, 179.
10. Mason, J. S.; Good, A. C.; Martin, E. J. *Curr. Pharm. Des* **2001**, *7*, 567.
11. Hahn, M. J. *Chem. Inf. Comput. Sci.* **1997**, *37*, 80.
12. Putta, S.; Lemmen, C.; Beroza, P.; Greene, J. *J. Chem. Inf. Comput. Sci.* **2002**, *42*, 1230.
13. Eyers, P. A.; Craxton, M.; Morrice, N.; Cohen, P.; Goedert, M. *Chem. Biol.* **1998**, *5*, 321.
14. *Catalyst*; Accelrys Inc., San Diego, CA.
15. Carson, M. *Methods Enzymol.* **1997**, *277*, 493.